Materials Science and Engineering C 55 (2015) 420–430

Contents lists available at ScienceDirect

Materials Science and Engineering C

journal homepage: www.elsevier.com/locate/msec

Improvement in glucose biosensing response of electrochemically grown polypyrrole nanotubes by incorporating crosslinked glucose oxidase

Pragya Agar Palod *, Vipul Singh

Molecular and Nanoelectronics Research Group (MNRG), Department of Electrical Engineering, Indian Institute of Technology Indore, Pithampur Auto Cluster Limited (PACL) Building, Survey No. 113/2-B, Village Hernia Khedi, Mhow, Indore, Madhya Pradesh, India

ARTICLE INFO

Article history:
Received 21 November 2014
Received in revised form 29 March 2015
Accepted 8 May 2015
Available online 12 May 2015

Keywords:
Glucose biosensor
Polypyrrole
Cross-linking
Glucose oxidase
Sensitivity
Porosity

ABSTRACT

In this paper a novel enzymatic glucose biosensor has been reported in which platinum coated alumina membranes (Anodisc™s) have been employed as templates for the growth of polypyrrole (PPy) nanotube arrays using electrochemical polymerization. The PPy nanotube arrays were grown on Anodisc™s of pore diameter 100 nm using potentiostatic electropolymerization. In order to optimize the polymerization time, immobilization of glucose oxidase (GO_x) was first performed using physical adsorption followed by measuring its biosensing response which was examined amperometrically for increasing concentrations of glucose. In order to further improve the sensing performance of the biosensor fabricated for optimum polymerization duration, enzyme immobilization was carried out using cross-linking with glutaraldehyde and bovine serum albumin (BSA). Approximately six fold enhancement in the sensitivity was observed in the fabricated electrodes. The biosensors also showed a wide range of linear operation (0.2–13 mM), limit of detection of 50 μM glucose concentration, excellent selectivity for glucose, notable reliability for real sample detection and substantially improved shelf life.

1. Introduction

Since the discovery of enzyme electrodes for glucose detection by Clark and Lyons in 1962, stimulated research augmented by increasing demand of portable glucose biosensors for treatment of diabetes have been carried out worldwide [1–3]. Though non-enzymatic biosensors are also being investigated, however, such biosensors suffer from poor selectivity due to large interferences from easily oxidizable electroactive species present in the blood. On the other hand, extraordinarily superior specificity and sensitivity of enzymes towards specific substrate molecules has encouraged accelerated research in the field of enzymatic glucose biosensors for various applications such as glucose monitoring for diabetes care, beverage and food industry, bioprocess monitoring, and drug discovery and analysis [4,5].

Conceptually, a biosensor incorporates two important components: a bio-recognition element (such as enzymes) and a transducer adjacent to it. The role of transducer is to sense the changes in the system as a consequence of the interaction between the substrate (analyte) and bio-recognition element (enzyme) [5]. Enzyme immobilization is an indispensable step in order to enable prolonged and repetitive use of biosensor with consistent biosensing response [6]. In this respect, as a transducer, conductive polymers (CPs) are materials of choice due to their excellent electronic properties and biocompatibility [4,7]. Among various CPs, one of the most studied polymers is polypyrrole (PPy) [8,9]. Due to high electronic conductivity, high environmental stability and inherent biocompatibility it provides a very suitable microenvironment for enzyme immobilization and signal transduction [8,10]. Owing to excellent solubility of pyrrole monomer in a broad range of aqueous as well as non-aqueous solvents and its low oxidation potential for electro-oxidation, electrochemical polymerization has been adopted as one of the most preferred methods for obtaining PPy thin films on conductive substrates [9,11–13].

CP nanostructures exhibit much higher specific surface area than their bulk counterparts leading to significant enhancement in their electrochemical activity [13–16]. Hence, manifold enrichment in the enzyme loading and subsequent interactions of enzyme with substrate molecules leads to improved sensitivity of biosensors [14,15,17]. Some of the well-known techniques for enzyme immobilization are physical adsorption, co-entrapment, cross-linking, covalent binding etc., each holding its own merits [5,18]. In our recent research work, PPy nanotubes had been grown over Pt coated Anodisc™s with 200 nm pore diameter, in which physical adsorption was employed for immobilization of GO_x [17]. However, it suffered from poor stability. Due to the involvement of weak Van der Waal forces, the enzymes immobilized via physical adsorption are very much prone to leach out of the support matrix [19]. Improvement in the shelf life of biosensor is of critical importance towards the realization of a practically useful biosensor [7,10]. Another popular method of immobilization is co-entrapment, which requires the enzyme molecules to be mixed with monomer solution. At a pH greater than its iso-electric point, enzyme bears a net negative charge and gets attached with the polycationic backbone of the growing

* Corresponding author.
E-mail address: agarpragya@gmail.com (P.A. Palod).

http://dx.doi.org/10.1016/j.msec.2015.05.038
0928-4931/

polymer film [20–22]. However, a major drawback of immobilization by co-entrapment is that it is very much sensitive to pH of the monomer solution and requires huge amounts of enzyme molecules for efficient enzyme loading [7]. Also due to most of the enzyme molecules are located deep in the polymer matrix, delayed interaction between enzyme and substrate molecules may lead to unfavorably large response times [20]. Immobilization by covalent binding provides efficient binding between enzyme and immobilizing material. However, it requires modification of sensor surface to acquire a reactive group for attachment with enzyme [23]. In contrast, immobilization by crosslinking of enzyme with the support matrix via some bi-functional crosslinking agent such as glutaraldehyde is a separate process similar to physical adsorption and a relatively small amount of enzyme is required as compared to co-entrapment. At the same time sensitivity and storage stability of the biosensor can be extended up to several times [24].

Template based method invented by Martin et al. has received considerable attention over the recent years mainly owing to its simplicity, controllability and widespread applications [25,26]. In the past decade, anodically oxidized alumina membranes (Anodisc™) have been extensively used as templates for the growth of nanotube and nanowire structures. The experimental parameters viz. monomer and supporting electrolyte concentrations, applied potential or current density, polymerization duration etc. determine whether nanotube or nanowire arrays are grown along the porous walls of the Anodisc™. Xiao et al. emphasized that low monomer concentration and high polymerization potential are crucial for the growth of polymer nanotubes [27]. Anodisc™s are commercially available with three standard pore diameters viz. 20, 100 and 200 nm. In order to get the benefit of quantum effects, it is highly desirable to choose as small dimension as possible. 20 nm pore diameter is not suitable for loading of GO_x due to restrictions imposed by the dimension (6.0 nm × 5.2 nm × 7.7 nm) of enzyme molecule [28,29]. Therefore, in this work, Anodisc™s with 100 nm pore diameter were employed in order to grow PPy nanotube arrays using potentiostatic electrochemical oxidation of pyrrole monomer. The fabricated electrodes were used as supporting matrix for GO_x immobilization. Polymerization time was optimized for the highest sensitivity for the fabricated biosensors. Realization of a novel biosensor with high sensitivity, selectivity, reproducibility and long storage life was the main objective of the presented work. In this regard, effect of two different immobilization techniques on the sensing response, selectivity towards glucose detection, shelf life and various other parameters has been studied for the optimum polymerization time for the fabricated biosensors using amperometric detection technique.

2. Experimental

2.1. Reagents

All required chemicals including pyrrole monomer, lithium perchlorate ($LiClO_4$), sodium phosphate dibasic (Na_2HPO_4), sodium phosphate monobasic (NaH_2PO_4), D-(+)-glucose, uric acid, L-ascorbic acid, ethanol, glucose oxidase from *Aspergillus niger* (E. C. 1.1.3.4), hydrogen peroxide (H_2O_2), glutaraldehyde, and bovine serum albumin (BSA) were used as obtained from Sigma-Aldrich. All the chemicals were of analytical grade. Anodisc™s (pore diameter: 100 nm) were purchased from Whatman. Deionized (DI) water of 18 MΩ resistivity was used for the preparation of aqueous solutions. A 50 mM phosphate buffer solution (PBS) of pH 6.8 was prepared using NaH_2PO_4, Na_2HPO_4 and DI water.

2.2. Apparatus

All electrochemical experiments including activity assay, electropolymerization and response current measurements were performed at room temperature in a three electrode electrochemical cell using electrochemical station (Autolab PGSTAT302N). Platinum foil and Ag/AgCl were used as counter and reference electrodes, respectively. The morphological characterization of the produced Pt and PPy films was performed using Field Emission Scanning Electron Microscope (FESEM, Carl Zeiss SUPRA55). The morphology of nanotubes was also studied by using Transmission Electron Microscope (TEM, FEI's Tecnai G^2 S-TWIN model) operated at 200 keV. In order to quantify the amount of enzyme loaded onto different PPy nanotube array electrodes, fluorescence emission spectra were recorded using Fluoromax-4p spectrofluorometer from Horiba Jobin Yvon (Model: FM-100). Structural analysis of native GO_x as well as GO_x immobilized using physical adsorption and cross-linking, was performed using Fourier Transform Infra-Red (FTIR) spectroscopy. In order to record the IR spectra, Tensor 27 (from Bruker) spectrometer was operated in the wave number range from 4000 to 500 cm^{-1}. Each spectrum was the resultant of average of 16 scans collected with 2 cm^{-1} resolution. Image processing tool of MATLAB (© 1984–2011 The MathWorks, Inc.) was employed to compute the surface porosity of Pt coated electrode before and after polymerization for different durations. Pore volumes of PPy nanotubes were also experimentally determined for different electrodes using Brunauer–Emmett–Teller (BET) analysis. Nitrogen adsorption–desorption isotherms were measured at 77 K using volumetric gas adsorption station (Quantachrome Autosorb 1C TCD Analyzer, Model: ASIC-X-TCD6).

2.3. Fabrication of electrodes

The schematic diagram shown in Fig. 1(a) illustrates the important steps followed for the fabrication of biosensors. Pt/Anodisc™ electrodes were obtained by depositing Pt on the masked Anodisc™s using direct current magnetron sputtering system operated at base pressure of 2×10^{-7} mbar. Pt was sputtered on the substrates rotated at a speed of about 30 rotations per minute (rpm) under the argon gas pressure of 5×10^{-3} mbar and a deposition rate of 1 Å-s^{-1}. During deposition argon gas flow rate was maintained at 20 cm^3-min^{-1}. Subsequently, electropolymerization was carried out under potentiostatic condition (1.8 V) in aqueous solution containing freshly distilled pyrrole monomer (25 mM) and $LiClO_4$ (100 mM). As a final step, the immobilization of GO_x resulted into a functional glucose biosensor. Fig. 1(b) shows the cross-sectional view of GO_x/PPy/Pt/Anodisc™ electrode. Nanoporosity of electrodes is the key requirement to realize significant improvements in the performance of the biosensor by means of enhancement in the surface-to-volume ratio [30]. Hence, the optimization of Pt thickness is critical in this regard. Optimum thickness of Pt for producing conducting surface and walls of template without hurting the porous nanostructures was obtained to be 50 nm. Polymerization duration was varied from 3 to 70 s for different samples.

2.4. Enzyme immobilization

2.4.1. Physical adsorption and quantification

Immobilization of enzymes to the surface of transducer is an essential step in order to localize them in the supporting matrix (which was the electrochemically grown PPy in our case) so as to extend their life for repetitive use. As required by the optimization of the polymerization time, enzymes were first immobilized by physical adsorption method. This simple method binds enzymes with a transducer via electrostatic interactions [18]. GO_x solution (10 mg-ml^{-1}) was prepared in 50 mM PBS (pH 6.8). Enzyme immobilization was carried out by placing 10 μl aliquot from GO_x solution onto PPy coated surface (PPy/Pt/Anodisc™) for physical adsorption and electrode was kept overnight in incubator at 4 °C. Before using the electrode for amperometric biosensing, it was washed carefully in PBS to do away with loosely adhered enzyme molecules. Electrodes were stored in incubator when not in use.

Polymerization time plays an important role in controlling (i) the coverage of Pt surface by PPy and (ii) porosity of the electrodes, which in turn affect the subsequent enzyme loading. The polymerization time corresponding to the highest enzyme loading indicates a perfect balance between the Pt surface coverage by PPy and electrode porosity

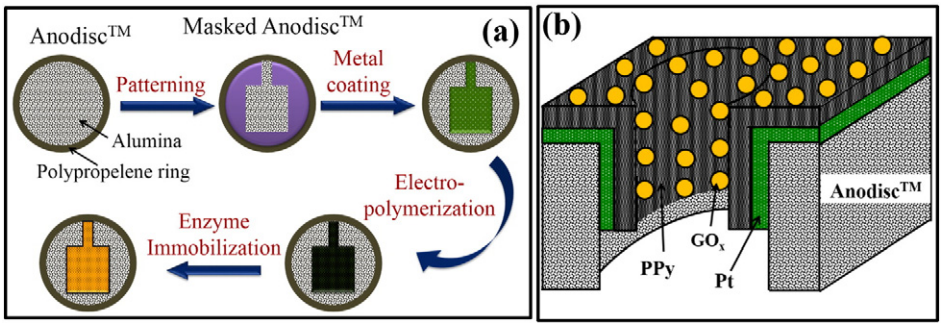

Fig. 1. Schematic showing (a) important steps of biosensor fabrication, (b) cross-sectional view of PPy/Pt/Anodisc™ electrode.

required for enzyme's movement into the PPy nanotubes. The electrodes fabricated for the optimum polymerization time were expected to result in the highest sensitivity. Therefore, in addition to amperometric detection, enzyme quantification is also a helpful tool for the purpose of the optimization of polymerization time.

Tryptophan present in each GO_x molecule is an aromatic residue, which contributes to the intrinsic fluorescence in this molecule. As the intensity of the fluorescence emission is directly proportional to the amount of enzyme used for the measurement. Therefore, the immobilized enzymes can be quantified using this optical characteristic of GO_x [17]. Excitation and emission wavelengths required for obtaining tryptophan fluorescence are 295 nm and 340 nm, respectively [31]. Excitation and emission slits were set at 2 nm each. Steady state fluorescence measured for known amounts of GO_x in PBS resulted into a plot for intensity versus amount of GO_x, which followed a linear relationship and thus, served as a calibration plot for the purpose of enzyme quantification. As known amount of GO_x (100 μg) was used for enzyme immobilization, PBS containing unadhered GO_x molecules collected (separately for individual electrodes) after physical adsorption step, served as sample solution for the fluorescence measurement. Amount of unadhered GO_x molecules was estimated by comparing the intensity values with calibration plot. Further, the subtraction of the corresponding values from 100 μg (total amount of enzyme used for immobilization) led to an estimate of loaded enzyme for each of the sensing electrodes.

2.4.2. Crosslinking

GO_x was immobilized via crosslinking of glutaraldehyde (as a bi-functional crosslinking agent) in the presence of BSA (as a protein stabilizer). Cross-linking solution was freshly prepared by mixing 10 μl glutaraldehyde solution (1 wt.%) and 10 μl BSA (from 50 mg-ml^{-1}) with 20 μl PBS. The solution was placed on PPy coated nanotube array electrode after physical adsorption step. After drying the electrode in air, it was kept in an incubator overnight for stabilization. Before using electrode for biosensing, it was immersed in PBS for removing molecules left unemployed in cross-linking.

2.5. Amperometric measurements on biosensor

Among various techniques known for enzymatic glucose detection, amperometric detection is the most preferred method due to its simplicity and accuracy [32]. The underlying principle for amperometric glucose detection is presented in Eqs. (1)–(3).

$$C_6H_{12}O_6 + GO_x(FAD) + H_2O \rightarrow C_6H_{12}O_7 + GO_x(FADH_2) \quad (1)$$

$$GO_x(FADH_2) + O_2 \rightarrow GO_x(FAD) + H_2O_2 \quad (2)$$

$$H_2O_2 \xrightarrow{0.7\,V} 2H^+ + 2e^- + O_2 \quad (3)$$

GO_x immobilized on the surface of transducer catalyzes oxidation of glucose ($C_6H_{12}O_6$) into gluconic acid ($C_6H_{12}O_7$). Flavin adenine dinucleotide (FAD), a redox cofactor residing in GO_x undergoes reduction and thus generates reduced form of enzyme ($GO_x(FADH_2)$), which subsequently, in the presence of molecular oxygen re-oxidizes to form $GO_x(FAD)$. Hydrogen peroxide (H_2O_2), a byproduct of this reaction decomposes into electrons and ions due to an applied potential of 0.7 V at an anode [1,5]. Therefore, current proportional to the glucose concentration flows in the circuit. Hence, the calibration of the biosensor device can be carried out in terms of the measured current.

Stock solution of 1 M glucose was prepared in DI water and allowed to mutarotate overnight before use in order to establish the equilibrium concentrations between α and β anomers [33]. Sensing electrode (GO_x/PPy/Pt/Anodisc™) placed in a three electrode electrochemical cell, was used as a working electrode. The electrodes were all immersed in PBS (50 mM, pH 6.8). A fixed potential of 0.7 V was applied to the working electrode, while the solution was stirred at a constant speed. After attaining a steady state background current, aliquots of glucose solution were added into the cell. Increments in current density upon successive additions of glucose were recorded against time.

Biosensor characteristics viz. sensitivity, response time, lower detection limit and linear range of operation were derived from the response curve.

2.6. Evaluation of Michaelis–Menten constant

From the study of steady state kinetics of the enzyme catalyzed reactions it is very well known that there exists a hyperbolic relationship between initial reaction rate (V_0) and the substrate concentration ([S]) [34]. The mathematical form of this relationship is given by Eq. (4) and is known as the Michaelis–Menten equation.

$$V_0 = \frac{V_{max} \times [S]}{K_m + [S]} \quad (4)$$

Here V_{max} is the limiting value of the initial reaction rate. K_m is Michaelis–Menten constant, which is numerically equal to the substrate concentration for which reaction rate attains half of its maximum value [34]. Evaluation of this constant is important as it gives information about affinity of enzymes for the specific substrate molecules. Smaller the value of K_m, stronger will be the affinity [35]. Based on various transformations of Eq. (4), several methods for the evaluation of K_m have been proposed in the literature, for example Lineweaver–Burk method, method of Hanes, and method of Eadie–Hofstee [34]. However linear transformations of enzyme kinetic data are subject to errors. Also, these methods require certain calculations to be performed on the transformed experimental data and are thereby subject to potential errors in the obtained results [34]. On the other hand, a graphical method pioneered by Eisenthal and Bowden presents a straight forward and simplistic way of estimating kinetic parameters requiring no

calculations to be performed [36]. This method employs following rearrangement of Eq. (4):

$$\frac{V_{max}}{V_0} - \frac{K_m}{[S]} = 1. \quad (5)$$

Eq. (5) presents equation of a straight line in $V_{max}K_m$ space with intercepts V_0 and $-[S]$, on the respective axes. i. e. for each observation (V_0, [S]) a straight line can be plotted with intercepts V_0 and $-[S]$. The point of intersection of the lines plotted for different observations (V_0, [S]) defines the unique values of V_{max} and K_m which satisfy the Eq. (5) for every observation. Due to possibility of errors in the experimental observations, it is likely to obtain multiple points of intersection (rather than a unique point). Therefore, the most appropriate values of V_{max} and K_m can be obtained by selecting the median for each of them [36].

3. Results and discussion

3.1. Enzyme activity assay

Enzymes are sensitive biomolecules with the folded tertiary structure. The environmental conditions viz. temperature, pH etc. may unfold it to a random polypeptide chain leading to the loss of the enzyme activity [34]. Hence, the determination of the specific activity of enzymes prior to their usage for immobilization purposes is of utmost importance. Specific activity refers to micro-moles of substrate converted into product per minute by enzyme contained in 1 mg protein [34]. Specific activity of GO_x was determined using a simple and straight forward electrochemical assay [37]. The details of the procedure are given elsewhere [17]. The specific activity was computed as 111 U-mg^{-1} (1 U = 1 μ-mole substrate conversion-minute^{-1}). This value falls well within the range (100–250 U-mg^{-1}) quoted by the manufacturer.

3.2. Optimization of polymerization time

3.2.1. Biosensing on electrodes with physically adsorbed GO_x

Glucose biosensing response was examined for the biosensors obtained for different polymerization durations (3–70 s). Amperometric response curve for the biosensor with polymerization time of 5 s has been shown in Fig. 2. Current response indicates the rate of oxidation of glucose by the GO_x immobilized in the PPy matrix. The step-like response of the biosensor for each successive addition of glucose is clearly evident in the section of the response curve shown in the inset in Fig. 2. Instantaneous rise in steady state current upon the injection of glucose signifies the retention of GO_x activity upon immobilization. Response time was estimated to be 13 s. A curve, relating the steady state current density with glucose concentration was derived from amperometric response curve, for each biosensor. Fig. 3 shows the calibration curves for the biosensors with polymerization times 3, 5, 10, 30 and 70 s, respectively. In each of these curves, current density rises linearly for lower concentrations of glucose and tends to saturate at higher concentrations. This behavior originates from the enzyme kinetics. At higher concentrations, occupancy of all active sites of enzymes by glucose molecules leads to saturated response [34]. Linear range of operation of biosensor was estimated by linear regression analysis of the plotted calibration curve.

For each fabricated biosensor, sensitivity was computed from the slope of the corresponding calibration curve. Sensitivity values obtained for the different biosensors have been shown in Fig. 4. The biosensor fabricated for the polymerization time of 5 s, resulted into the highest sensitivity of 12.3 mA-cm^{-2}-M^{-1}, over an extended linear range of operation (0.5–17 mM) and the limit of detection of 50 μM. Other than this polymerization time (5 s), for both, increased as well as decreased polymerization durations, sharp decline in the sensitivity values of the biosensors was observed. Further analysis of the obtained biosensor response was essential in order to clearly ascertain the

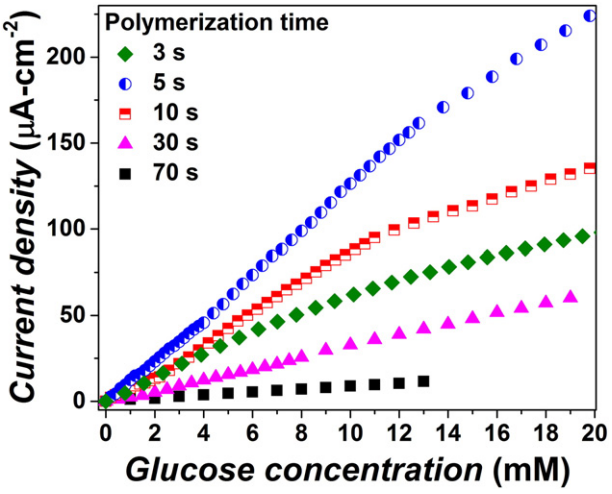

Fig. 3. Calibration curves for biosensors with polymerization time 3, 5, 10, 30 and 70 s.

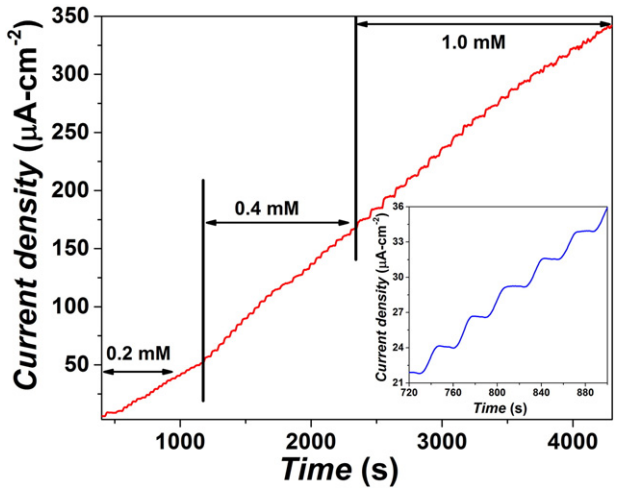

Fig. 2. Amperometric response curve for the biosensor with polymerization time 5 s obtained from immobilization via physical adsorption. A part of the response curve in inset, shows step like response.

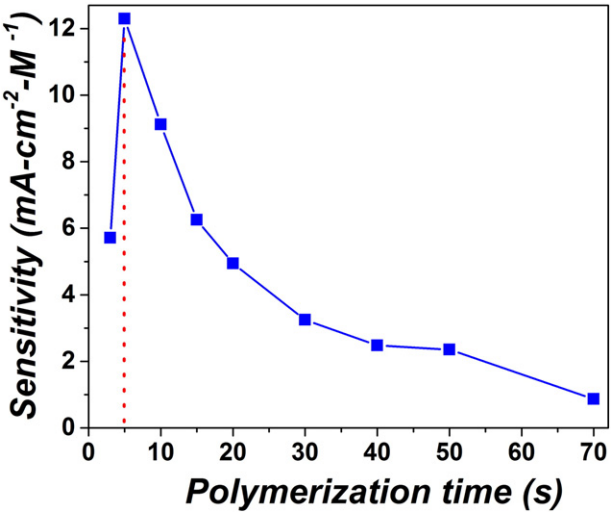

Fig. 4. Variation in sensitivity values (for biosensor with physically adsorbed GO_x) with polymerization time from 3–70 s.

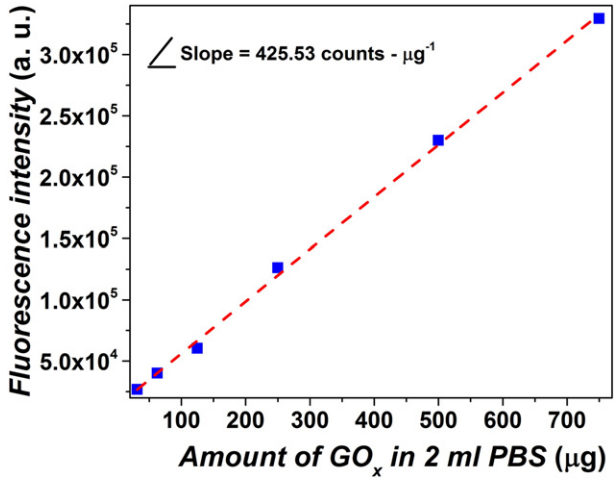

Fig. 5. Calibration plot for the quantification of immobilized enzymes, using fluorescence measurement.

reasons for observed optimized sensitivity of the biosensor corresponding to the electrochemical polymerization time of 5 s.

Fig. 5 shows the calibration plot obtained from fluorescence measurements performed for known amounts of GO_x dissolved in PBS, against which the intensity values obtained for different sample solutions, were compared. The values of immobilized enzymes for different polymerization durations, calculated from fluorescence studies have been shown in Fig. 6. Maximum loading of GO_x was obtained corresponding to polymerization time of 5 s. This result is in agreement with the highest sensitivity observed for 5 s polymerization duration. In this case, the largest number of GO_x molecules present in the polymer matrix led to increased sensitivity in the biosensor for the injected glucose.

3.2.2. FESEM characterization of electrodes and porosity analysis

Surface characterization of Pt electrode and grown PPy films was carried out using FESEM. Fig. 7(a) shows the top view FESEM image of Anodisc™ after Pt deposition. As evident from the micrograph, the surface was coated with the spherical nanoparticles of size less than 40 nm. Fig. 7(b–e) shows FESEM images of the electrodes after electrochemical polymerization for durations 5, 10, 15 and 20 s, respectively. As evident from the micrographs, electrodes retained sufficient porosity till the polymerization time 5 s, after which the nanoporous structure of the

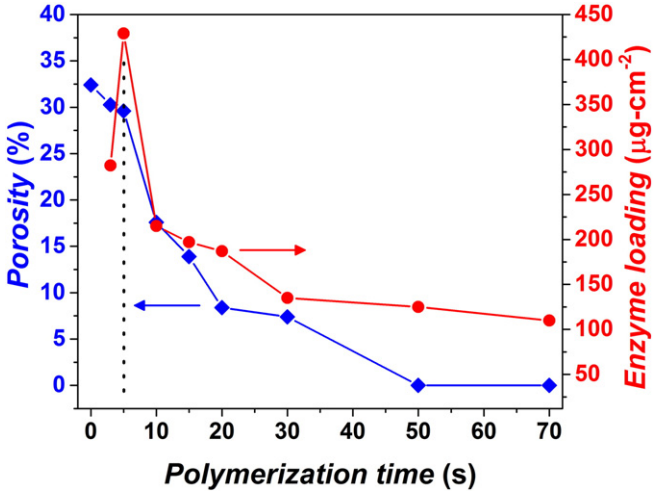

Fig. 6. Calculated values of porosity (blue curve) and amount of enzyme loaded per unit area of electrode (red curve) for biosensor with physically adsorbed GO_x for different polymerization times (3–70 s).

electrode surfaces was observed to diminish continuously with increasing the polymerization time. Eventually, no porous structure could be identified in the FESEM images of electrodes (not shown here) for the polymerization durations higher than 20 s.

This observation was further confirmed by calculating the porosity values (using MATLAB) for different electrodes. The analysis was performed by transforming the gray scale images obtained from FESEM into corresponding binary images (exhibiting only black and white regions; black regions representing the pores on the electrode). Porosity of the Pt coated and PPy modified electrodes was estimated by calculating the ratio of area covered by black pixels to the total area of the image (black + white). As shown in Fig. 6, porosity of Anodisc™ after Pt deposition was calculated to be slightly more than 32%. As polymerization was carried out successively for higher time durations, porosity of electrodes dropped due to PPy deposition inside the pores. Electrode held up to 29.6% porosity for polymerization time 5 s, after which noticeable drop in porosity was recorded. Eventually, for 50 s polymerization time pores were more or less completely blocked by deposited PPy film, leading to non-porous structures.

Length of the PPy nanotubes plays an important role in determining the magnitude of enhancement in surface-to-volume ratio. Sample was prepared separately so as to estimate the length of nanotubes. After polymerization, PPy nanotubes were uncovered by dissolving the Anodisc™ carefully in 1 M NaOH solution and washing the remaining electrode thoroughly with copious amounts of DI water, after which the sample was dried under a vacuum [38]. As shown in the cross-sectional view of the nanotubes in Fig. 7(f), the measured length of the nanotubes was approximately 650 nm. A rough calculation of surface area enhancement (under the assumption that lengths of nanotubes are uniform) was performed using the following formulae:

$$\text{Area of plane electrode with radius r, } A_{bulk} = \pi r^2 \tag{6}$$

$$\text{Area of nanoporous electrode with radius r, } A_{nano} = 2\pi rh \tag{7}$$

where h is length of the cylindrical nanopore.

$$\text{Area enhancement factor, } A_{nano}/A_{bulk} = 2h/r. \tag{8}$$

For pore density of roughly 30% (quoted by manufacturer),

$$A_{nano}/A_{bulk} \cong 0.7 + 0.3(2h/r). \tag{9}$$

Substitution of values of h (=650 nm) and r (=50 nm, for 100 nm pore diameter), in Eq. (9) results in approximately 8.5 times enhancement in the surface area.

The obtained FESEM images and Fig. 6 suggest that the growth of PPy film on the surface and porous walls of the electrode was governed by the progressive nucleation and growth model according to which, PPy nodules nucleated in the early stages of potentiostatic electropolymerization, grew three dimensionally and subsequently merged so as to form larger polymer aggregates [39,40]. The analysis suggests that minimum time required for complete coverage of Pt surface by PPy film is 5 s, below which limited area of PPy available for enzyme loading resulted in poor sensing response as shown in Fig. 4. For optimum polymerization time (5 s), owing to increased Pt surface coverage by PPy film along with reasonably good porosity, GO_x loading during immobilization was encouraged as evident from Fig. 6. Thus, maximum amount of immobilized GO_x resulted in the highest sensitivity of 12.3 mA-cm^{-2}-M^{-1} for this biosensor. The thickness of grown PPy is proportional to the total amount of the charge associated with pyrrole oxidation per unit area of electrode [41]. Growth of thicker PPy films, for higher polymerization durations (>5 s), shrinks the pores as the inner walls of PPy nanotubes approach closer. It consequently reduces the surface area available for enzyme loading and also raises the incompatibility between pore size and molecular dimensions of

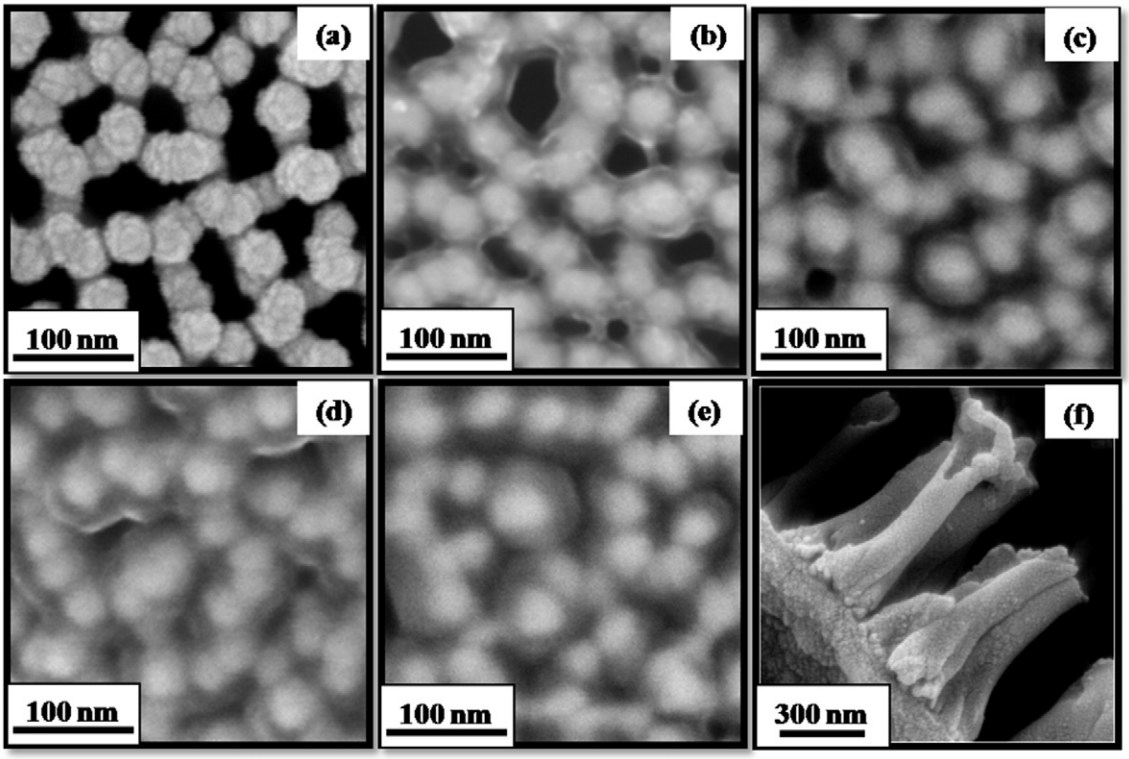

Fig. 7. FESEM top view images of (a) 50 nm Pt coated Anodisc™, electrode after polymerization for (b) 5 s, (c) 10 s, (d) 15 s, (e) 20 s time, and (f) cross-sectional view of PPy nanotubes after removal of Anodisc™.

the enzyme (Figs. 6 and 7). For polymerization time 30 s, resulted from the pronounced clogging of pores, the sensitivity reduced to a value approximately one fourth of its maximum, indicating the enzyme immobilization more or less limited to the surface of the electrode. The above analysis validates dependence of the sensitivity upon two factors: (i) Amount of immobilized GO_x and (ii) porosity of the electrode. An appropriate balance between the Pt surface coverage by PPy and electrode porosity for the optimum polymerization time of 5 s resulted in highest sensitivity for this biosensor.

Nitrogen adsorption analysis was performed on the surfaces of electrodes fabricated for different polymerization times. Before each measurement, the sample was degassed at 100 °C temperature for 2 h. The nitrogen adsorption isotherms were measured at 77 K, on the three electrodes fabricated for polymerization times 5, 15 and 20 s, respectively (Fig. S1). The value of specific pore volume has been determined from the amount of vapor adsorbed on the surface of adsorbent [42,43]. For three polymerization times 5, 15 and 20 s, the values of specific pore volume, extracted from adsorption isotherms, using the BET equation, were found to be equal to 1.649, 1.362 and 1.343 cm^3-g^{-1}, respectively. Thus, the electrode surface corresponding to polymerization time of 5 s, yielded the highest pore volume (1.649 cm^3-g^{-1}). Accordingly, the electrode surface was found to have maximum adsorption capacity for this polymerization time. The BET analysis further confirmed that the polymerization time of 5 s was optimum to provide maximum enzyme loading owing the highly porous electrode configuration.

3.2.3. Identification of core–shell structures using TEM characterization

In order to identify the core–shell structures, electrode surface for the optimized polymerization time of 5 s, was characterized using TEM. Prior to characterization, alumina was dissolved in the way similar to that for the estimation of length of nanotubes as discussed in previous section. The dried samples were then dispersed in ethanol by ultrasonication. Definite volume of the obtained dispersion was then placed on the TEM grid, which after evaporation of ethanol was mounted on the grid holder for the characterization. Fig. 8(a) and (b)

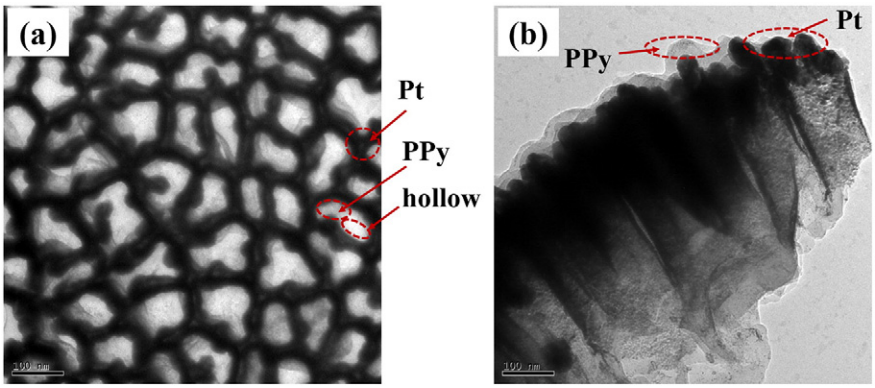

Fig. 8. TEM (a) top-view and (b) cross-sectional images of electrode surface for polymerization time of 5 s.

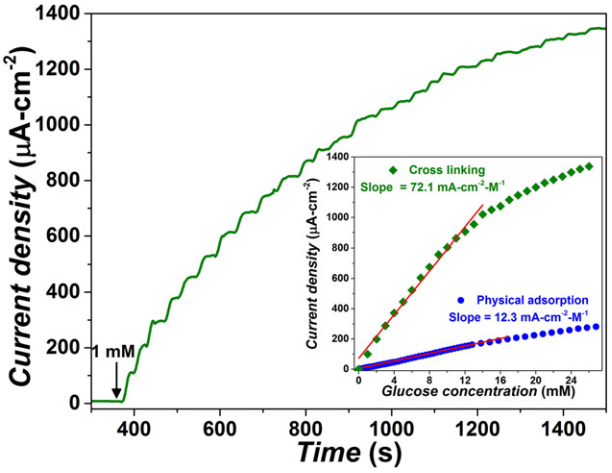

Fig. 9. Amperometric response curve for the biosensor with optimum polymerization time (5 s) obtained by immobilization via cross-linking. Inset shows a comparison between calibration curves for biosensors obtained from immobilization via cross-linking and physical adsorption.

shows the corresponding top and cross-sectional views respectively. The existence of different phases has been verified from the high contrast among different regions. As marked in Fig. 8(a) and (b), the darkest region corresponded to the region covered by Pt (whose thickness was 50 nm), the grayish region corresponded to the PPy film, while the lightest region in the middle of each nanotube (Fig. 8(a)) corresponded to the hollow region of the nanotube.

3.3. Improvement in the performance of biosensor by cross-linking of enzymes

Though optimization of polymerization time yielded maximum sensitivity for physically adsorbed GO_x enzyme molecules; however, the fabricated biosensor lost 73.6% of its sensitivity after storage of 12 days. The observed decay in the sensitivity has been attributed to the substantial leaching of the adsorbed GO_x molecules out of the support matrix due to weak van der Waal forces involved [30]. Improvement in the storage stability is one of the key requirements in order to develop practically useful biosensors. Further, the amount of enzyme molecules is restricted to one monolayer in the case of physical adsorption [19]. Therefore the use of some other immobilization techniques, incorporating enzymes in CP matrix with stronger binding forces is highly desired. In this regard, cross-linking has emerged out to be a powerful technique for enzyme immobilization [24].

3.3.1. Sensing response

Biosensing response of the electrode obtained by cross-linking of GO_x was recorded in a way similar to that for biosensor obtained from physical adsorption. Fig. 9 shows the sensing response curve for the newly fabricated biosensor for the optimum polymerization time.

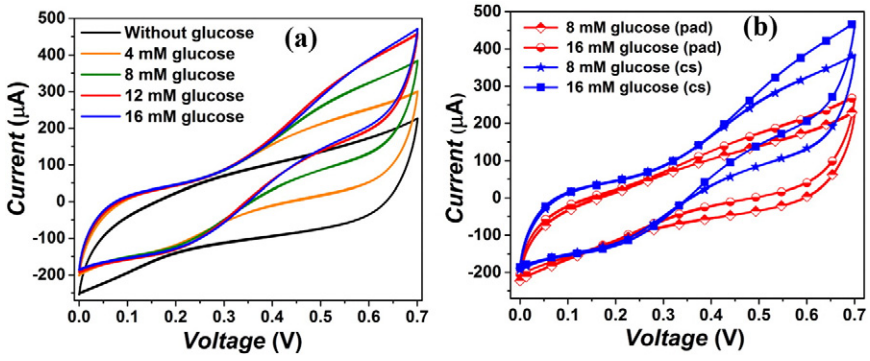

Fig. 10. (a) Cyclic voltammetric response of biosensor with cross-linked GO_x for different concentrations of injected glucose. Applied scan rate was 100 mV-s^{-1}. (b) Comparison between cyclic voltammetric responses of the biosensors for physically adsorbed (pad) and cross-linked (cs) GO_x for two concentrations (8, 16 mM) of injected glucose.

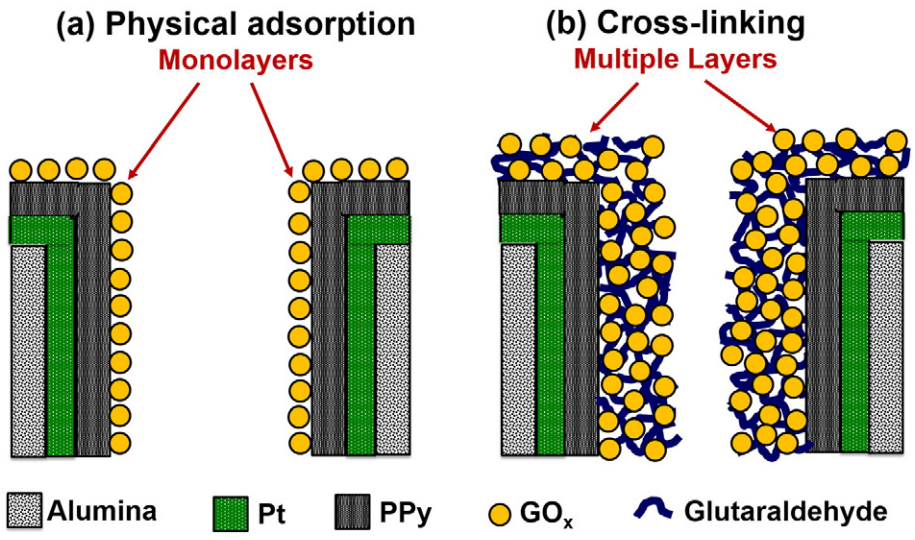

Fig. 11. Schematic views of cross-sections of the nanotube (PPy/Pt/Anodisc™) electrodes for the enzyme immobilization using two methods: (a) physical adsorption and (b) cross-linking.

Instantaneous rise in current confirms the non-denaturing of enzymes upon cross-linking. Calibration curve for the fabricated biosensor originated from the response curve has been compared with that obtained from physical adsorption of GO_x. As shown in the inset of Fig. 9, the newly fabricated biosensor exhibited an excellent sensitivity of 72.1 mA-cm^{-2}-M^{-1} with a linear range of operation extending from 0.2 to 13 mM. Thus, the sensitivity of biosensor increased for almost 6 times (to that from physical adsorption) by the immobilization of GO_x using cross-linking. It implies that cross-linking greatly enhanced the enzyme loading by means of the covalent bond formation among enzyme, cross-linking agent and glutaraldehyde. No change in the response time was detected.

3.3.2. Cyclic voltammetry studies

Further, the study of glucose oxidation reactions catalyzed by GO_x immobilized onto the PPy matrix of biosensing electrode, was performed using cyclic voltammetry (CV). Fig. 10(a) shows the cyclic voltammograms recorded for the biosensor corresponding to optimized polymerization time of 5 s, with cross-linked GO_x. Applied scan rate was 100 mV-s^{-1}. As evident from the figure, in comparison to the background current obtained in the absence of glucose, a clear increase in the oxidation current was observed upon the addition of glucose. Current values were found to increase upon increasing the glucose concentration from 4 mM to 16 mM. This result was a further confirmation of GO_x catalyzed glucose oxidation. Fig. 10(b) shows a comparison between the cyclic voltammetric responses of the biosensors obtained by two immobilization techniques, for two different concentrations of injected glucose. As shown in Fig. 10(b), for the two concentrations of glucose (8, 16 mM), significantly enhanced current values obtained in the case of cross-linked GO_x supports the argument that cross-linking resulted into manifold enhancements in the enzyme loading, compared to the case of physically adsorbed GO_x. It is well known that the amount of immobilized enzyme molecules is usually restricted to one monolayer in the case of physical adsorption [19]. The schematic diagram shown in Fig. 11 demonstrates the cross-sections of the fabricated nanotube (GO_x/PPy/Pt/Anodisc™) electrodes for the enzyme immobilization performed using two methods: (a) physical adsorption and (b) cross-linking. The observed improvement in the sensitivity of the biosensor, upon cross-linking of GO_x, has been attributed to the improved enzyme loading resulted from the covalent bond formation among GO_x, glutaraldehyde and PPy matrix [44].

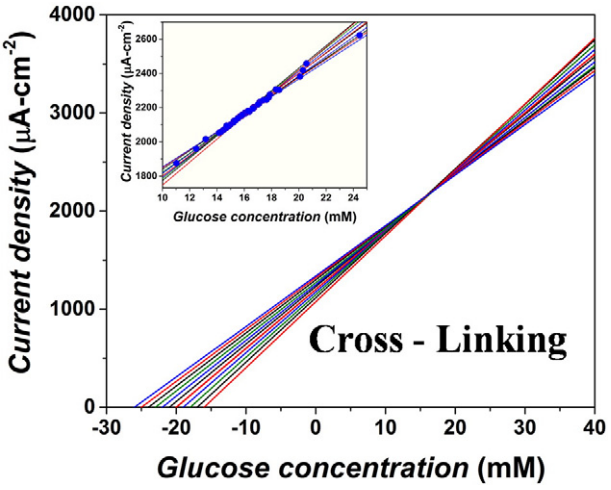

Fig. 13. Direct linear plot for determination of Michaelis–Menten constant for enzymes immobilized via cross-linking method. Inset shows intersections between various lines (blue dots showing points of intersection).

3.3.3. Michaelis–Menten constant

Change in the current density upon glucose injection is dictated by the enzyme kinetics. The calibration curves (as shown in Fig. 3 and inset of Fig. 9) exhibit the characteristics analogous to Michaelis–Menten curve (as already discussed in Section 2.6) [45]. Therefore analysis of Michaelis–Menten constant was performed by substituting the current density for initial reaction rate (V_0). Fig. 12 shows the direct liner plot obtained by drawing straight lines for a number of glucose concentration values and corresponding response current density values for biosensor obtained by physical adsorption of GO_x. The blue dots in the inset in Fig. 12 illustrate the points of intersection between the drawn lines. Similar exercise was carried out for the biosensor obtained by cross-linking of GO_x. Fig. 13 shows the corresponding direct linear plot, with inset showing a distribution of points of intersection (blue dots) of drawn lines. The computation of median (of distributions of points of intersection) for each case, resulted into the values of K_m as: 65.2 mM (physical adsorption) and 15.6 mM (cross-linking). The obtained values of K_m are in agreement with the observed sensing performances in the two cases. The enzymes immobilized via cross-linking were, thus found to exhibit much stronger affinity towards substrate

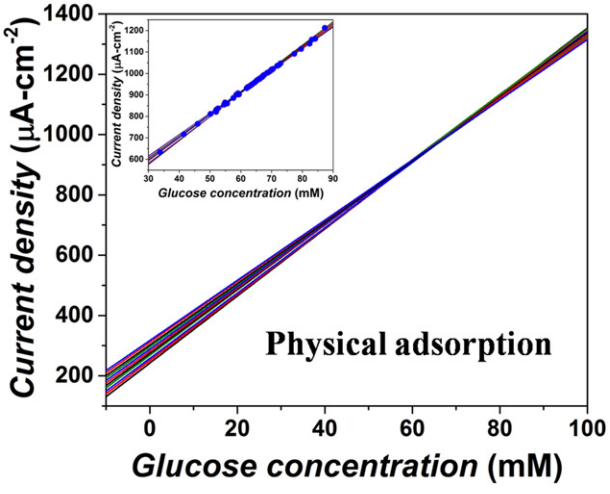

Fig. 12. Direct linear plot for determination of Michaelis–Menten constant for enzymes immobilized via physical adsorption method. Inset shows intersections between various lines (blue dots showing points of intersection).

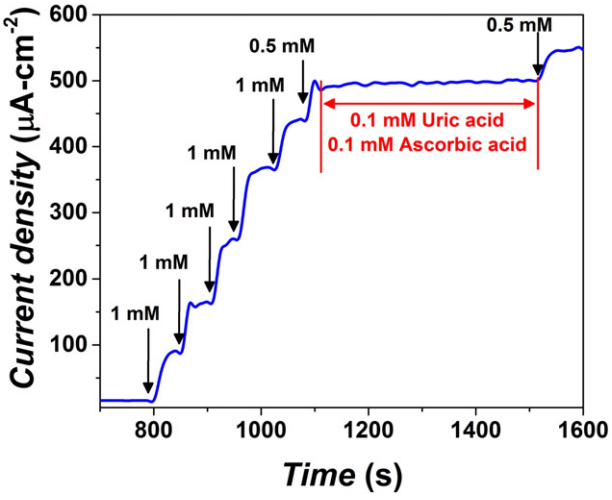

Fig. 14. Influence of electroactive interferents (uric acid, ascorbic acid) on biosensor response.

Table 1
Comparison of present work with recently reported similar glucose biosensors.

S. no.	Sensing matrix	Sensitivity (mA-cm^{-2}-M^{-1})	Linear range (mM)	Response time (s)	Reference
1	Anodisc™/Pt/PPy/GOx nanotube arrays	72.1	0.25–13	13	This work
2	Anodisc™/Pt/PPy/GOx nanotube arrays	7.4	0.5–13	3	2008 [20]
3	GOx/DAR-CS/PB-MWNTs*	77.9	0.01–1.1	10	2012 [47]
4	PPy/GOx nanowire arrays	9.97	0.1–8	7	2012 [48]
5	GOx/Pt-DENs/PANI/MWNTs†	42	0.001–12	5	2009 [49]
6	Pt NPs[a]-PANI[b] hydrogel	96.1	0.01–8	3	2013 [50]
7	GOx-PANI–Pectin NPs	79.5	0.06–4	–	2014 [51]

* GOx and diazoresin-chitosan on Prussian blue deposited multi-walled carbon nanotubes.
† Multi-walled carbon nanotubes coated with polyaniline and dendrimer-encapsulated Pt nanoparticles.
[a] Nanoparticles.
[b] Polyaniline.

(glucose) molecules and thus justify the extraordinary performance exhibited by the biosensor in that case.

3.3.4. Reproducibility, storage stability, interference study and real sample analysis

Three biosensors fabricated independently, showed acceptable reproducibility with a relative standard deviation (R. S. D.) of 5.4%.

The biosensors retained more than 92% of its sensitivity after storage for 20 days.

Interference effect from the easily oxidizable species normally present in the human blood, viz. uric acid and ascorbic acid was examined. As shown in Fig. 14, glucose concentration was first increased step-wise up to 5.5 mM (physiological concentration of glucose in the blood of healthy person) in the electrochemical cell set-up similar to the one used for sensing response studies. After that ascorbic acid and uric acid were injected sequentially so as to result in a final concentration of 0.1 mM for each of them, which is their physiological concentration in the human blood. As apparent in the figure, the biosensor responded in a very subdued manner for these interferents. In the response curve, a rise of barely 1.9% could be observed with respect to the response current density at 5.5 mM concentration of glucose. As evident in the figure, the biosensor responded in usual manner for the subsequent injections of glucose. This study ascertains the selectivity of the reported biosensor for diagnosis of glucose.

Reliability of the fabricated biosensor for practical applications was investigated by assaying glucose present in whole blood samples. Definite volumes of freshly obtained human whole blood samples were injected in electrochemical cell filled with PBS. Glucose concentrations in the two samples were measured using the biosensor and the evaluated values were compared with those, estimated by standard GOD–POD colorimetric assay [46]. The values obtained from biosensor (value obtained from standard assay, % deviation) were found to be: 12.37 mM (12.15 mM, 1.8%) and 4.5 mM (4.3 mM, 4.6%), respectively. Thus, the obtained values were found to be in good agreement with the values resulted from standard assay. Further, the validity of biosensor was confirmed by spiking the blood serum sample with standard glucose solution with known concentration (Fig. S2). The biosensor exhibited a recovery of 113% for the spiked blood serum sample.

3.3.5. Comparison with recently reported glucose biosensors

With the aim of evaluation of performance of the fabricated biosensor, some of its important characteristics have been compared in Table 1 with biosensors reported by various groups in recent years, in which functional nanomaterials (viz. carbon nanotubes, nanoparticles etc.) have been employed as immobilization matrix [20,47–51]. The developed biosensor has demonstrated excellent sensitivity and extended linear range of operation with reasonable response time.

3.4. Structural analysis of GO_x

GO_x, being a protein, comprises of a number of amino acids. The arrangement of various amino acid residues into sheets, helices etc. determines the complex structure and activity of the enzyme [52]. Conformation of enzyme is very much sensitive to its environment. Hence, upon immobilization, the conformational changes in the structure of GO_x, with respect to the native GO_x, were studied using FTIR. In the FTIR spectra of proteins, the vibrational modes of the amide group are very sensitive to the protein conformation. Out of various characteristic bands originating from the vibrations of the amide groups of protein, the secondary structure of protein is reflected by the amide I and amide II bands [53]. The amide I band (1700–1600 cm^{-1}) originates from the C═O stretching vibration, while amide II band (1600–1500 cm^{-1}) originates from the N–H in-plane bending [54].

Fig. 15 shows the FTIR spectrum of native and immobilized (physical adsorption and cross-linking) GO_x in the wave number range 1500–1700 cm^{-1}. The two absorption bands centered between 1660 and 1645 cm^{-1} (amide I) and 1550 and 1530 cm^{-1} (amide II) were obtained. As evident from Fig. 15, the intensity of absorption in the case of cross-linked GO_x was quite higher than that of physically adsorbed GO_x. This evidence is in agreement with the observed much higher sensitivity in the earlier case, which has been attributed to higher enzyme loading in case of cross-linking.

In order to get quantitative information about the secondary structure components, further analysis of amide I band was performed, as it is one of the most sensitive probes for the determination of protein secondary structure [53]. Second derivative spectra were computed to reveal the "hidden" bands in the original spectra. Fourier self-deconvolution (FSD) of the infrared spectra covering the amide I region was performed. Deconvolution was performed using Voigt function (a combination of Gaussian and Lorentzian functions) and the positions (in cm^{-1}) of the maxima in the fitted bands were obtained from the

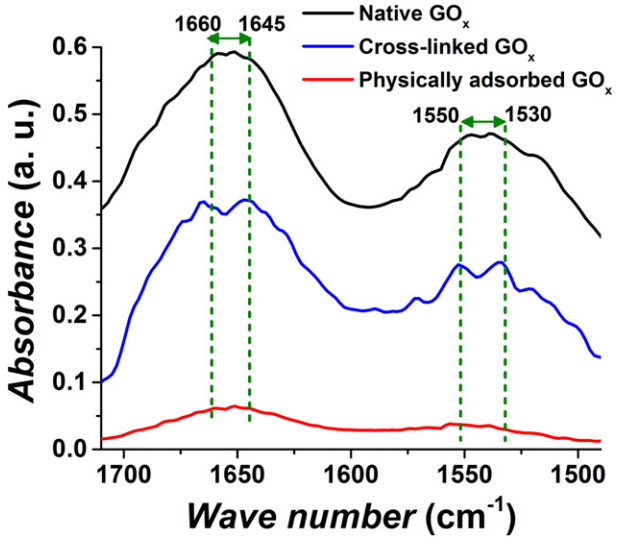

Fig. 15. FTIR spectrum of native and immobilized (physical adsorption and cross-linking) GO_x in the wave number range 1500–1700 cm^{-1}.

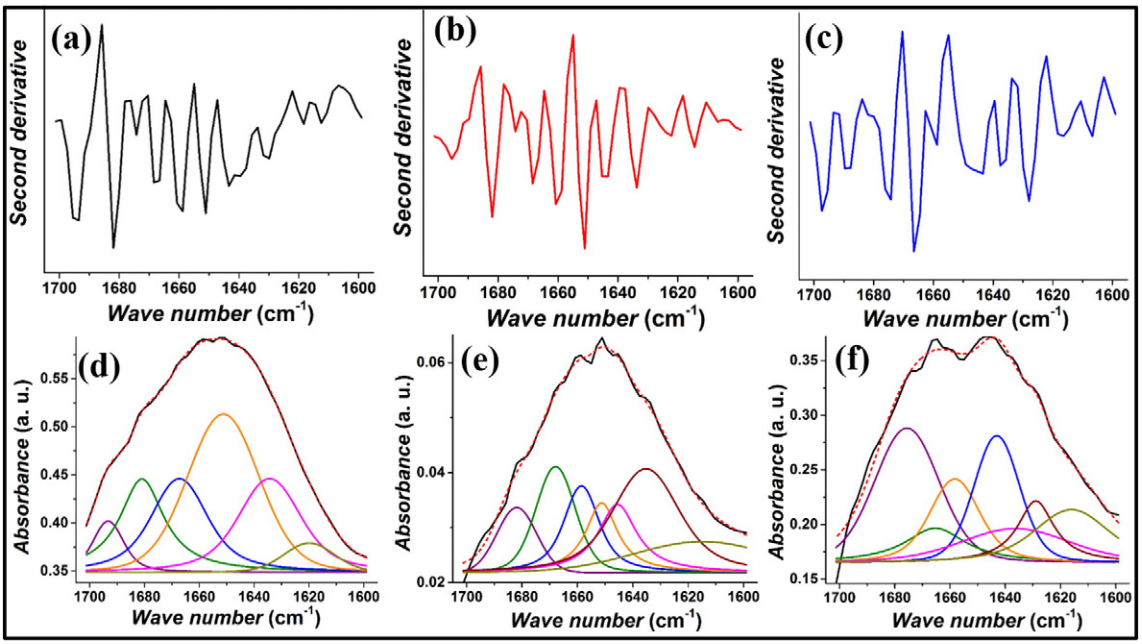

Fig. 16. Second derivative spectra (a, b, c) and the deconvoluted amide I spectra for the native, physically adsorbed and cross-linked GO_x (d, e, f), respectively.

respective positions of the minima in the second derivative spectra of the original spectra. A cumulative curve was generated to fit the original curve, for which the peak positions, widths and heights of the constituent curves were adjusted iteratively [54–56]. Fig. 16 shows the second derivative spectra (a, b, c) and the deconvoluted amide I spectra for the native, physically adsorbed and cross-linked GO_x (d, e, f), respectively. The bands at 1650–1660 cm^{-1} have been assigned to α-helices, at 1620–1640 cm^{-1} to β-sheets, at 1660–1685 cm^{-1} to β-turns, while the bands at 1610–1620 and 1685–1695 cm^{-1} have been designated to antiparallel β-sheets and the bands at 1640–1650 cm^{-1} to random coil structures [54,57]. The individual secondary structure elements were quantified by dividing the area occupied by each band by the total amide I area. The estimated secondary structure elements (%) have been reported in Table 2. The immobilization was found to result in significant reduction in the α-helix structures, which was more pronounced in the case of cross-linked GO_x, while the incremental changes in the β-sheets and β-turns were found to be relatively insignificant in case of cross-linked GO_x, when compared to physically adsorbed GO_x. Further, antiparallel β-sheets were observed to increase as a result of immobilization in both the cases. Also, immobilization was found to result in random coils, while it was found to be absent in the native GO_x. Despite the observed conformational changes in the secondary structure of cross-linked GO_x, observed extraordinarily high sensitivity of the biosensors incorporating cross-linked GO_x signified that the abundance of the immobilized GO_x played a more dominant role in the overall performance of the biosensor.

Table 2
Secondary structure elements (%) of GOx in different environments, determined by FTIR.

S. no.	Glucose oxidase (GOx)	α-Helix	β-Sheet	β-Turn	Anti-parallel β-sheet	Random coil
1	Native	34.0	20.0	36.2	9.8	–
2	Physically adsorbed	23.8	26.6	23.0	14.4	12.3
3	Cross-linked	13.7	21.2	34.2	13.7	17.3

4. Conclusions

In this report a novel biosensor has been demonstrated based on PPy nanotubes. It has been established that the nanoporosity of electrodes is the key requirement to bring about substantial improvements in the polymerization, enzyme loading and biosensing performance. Polymerization time was found to have a strong influence on the enzyme loading. Immobilization by cross-linking of GO_x has proven to be very effective towards improvement in the enzyme–substrate affinity, sensing response and shelf life of the biosensor, which is critical from the commercial point of view. Optimum polymerization time of merely 5 s is fully capable in producing biosensor operative over an extended linear range of 0.2–13 mM enabling the usage of this device for monitoring of diabetes and other applications requiring detection of high glucose concentrations as well.

Acknowledgement(s)

One of the authors, P. A. P. is grateful to Sophisticated Instrument Centre, IIT Indore for providing necessary research facilities. P. A. P. would like to thank Dr. Mukul Gupta (University Grants Commission Department of Atomic Energy (UGC-DAE) Consortium for Scientific Research Indore (M. P.), India) for the usage of dc Magnetron Sputtering System. She would like to thank Prof. B. R. Mehta (Professor, Department of Physics, IIT Delhi) for providing access to TEM characterization facility and Dr. S. Murugavel (Associate Professor, Deptartment of Physics and Astrophysics, University of Delhi , Delhi) for providing access to Nitrogen Sorption System for porosity analysis. P. A. P. would further like to thank Ministry of Human Resource and Development (MHRD), India for providing the Teaching Assistantship (TA). Author, V. S. would like to thank director of IIT Indore for providing constant support and encouragement for research.

Appendix A. Supplementary data

Supplementary data to this article can be found online at http://dx.doi.org/10.1016/j.msec.2015.05.038.

References

[1] L.C. Clark, C. Lyons, Electrode systems for continuous monitoring in cardiovascular surgery, Ann. N. Y. Acad. Sci. 102 (1962) 29–45.
[2] J.D. Newman, A.P.F. Turner, Home blood glucose biosensors: a commercial perspective, Biosens. Bioelectron. 20 (2005) 2435–2453.

[3] S. Wild, G. Roglic, A. Green, R. Sicree, H. King, Global prevalence of diabetes: estimates for the year 2000 and projections for 2030, Diabetes Care 27 (2004) 1047–1053.
[4] J. Wang, Electrochemical glucose biosensors, Chem. Rev. 108 (2008) 814–825.
[5] M.I. Prodromidis, M.I. Karayannis, Enzyme based amperometric biosensors for food analysis, Electroanalysis 14 (2002) 241–261.
[6] M. Singh, P.K. Kathuroju, N. Jampana, Polypyrrole based amperometric glucose biosensors, Sensors Actuators B Chem. 143 (2009) 430–443.
[7] N.K. Guimard, N. Gomez, C.E. Schmidt, Conducting polymers in biomedical engineering, Prog. Polym. Sci. 32 (2007) 876–921.
[8] Rajesh, S.S. Pandey, W. Takashima, K. Kaneto, Development of an amperometric biosensor based on a redox-mediator-doped polypyrrole film, J. Appl. Polym. Sci. 93 (2004) 927–933.
[9] K. Gurunathan, A.V. Murugan, R. Marimuthu, U.P. Mulik, D.P. Amalnerkar, Electrochemically synthesised conducting polymeric materials for applications towards technology in electronics, optoelectronics and energy storage devices, Mater. Chem. Phys. 61 (1999) 173–191.
[10] J.-C. Vidal, E. Garcia-Ruiz, J.-R. Castillo, Recent advances in electropolymerized conducting polymers in amperometric biosensors, Microchim. Acta 143 (2003) 93–111.
[11] Cosnier, S. and Karyakin, A. (2010) Electropolymerization: Concepts, Materials and Applications. ed. Wiley-VCH Verlag GmbH & Co. KGaA Germany.
[12] G.G. Wallace, G. Tsekouras, C. Wang, Electropolymerization, Wiley-VCH Verlag GmbH & Co. KGaA 2010, pp. 215–240.
[13] J. Huang, K. Wang, Z. Wei, Conducting polymer nanowire arrays with enhanced electrochemical performance, J. Mater. Chem. 20 (2010) 1117–1121.
[14] C. Li, H. Bai, G. Shi, Conducting polymer nanomaterials: electrosynthesis and applications, Chem. Soc. Rev. 38 (2009) 2397–2409.
[15] E.M.I.M. Ekanayake, D.M.G. Preethichandra, K. Kaneto, Polypyrrole nanotube array sensor for enhanced adsorption of glucose oxidase in glucose biosensors, Biosens. Bioelectron. 23 (2007) 107–113.
[16] V.S. Pragya Agar Palod, Facile synthesis of high density polypyrrole nanofiber network with controllable diameters by one step template free electropolymerization for biosensing applications, Sensors Actuators B Chem. 209 (2015) 85–93.
[17] P. Palod, S. Pandey, S. Hayase, V. Singh, Template-assisted electrochemical growth of polypyrrole nanotubes for development of high sensitivity glucose biosensor, Appl. Biochem. Biotechnol. (2014) 1–14.
[18] R.A. Sheldon, Enzyme immobilization: the quest for optimum performance, Adv. Synth. Catal. 349 (2007) 1289–1307.
[19] T. Ahuja, I.A. Mir, D. Kumar, Rajesh, Biomolecular immobilization on conducting polymers for biosensing applications, Biomaterials 28 (2007) 791–805.
[20] E.M.I. Ekanayake, D.M.G. Preethichandra, K. Kaneto, Effect of Glucose Oxidase Immobilizing Techniques on Performances of Nanoscale Polypyrrole Glucose Biosensors, 47 (2008) 1321–1324.
[21] S. Cosnier, Biomolecule immobilization on electrode surfaces by entrapment or attachment to electrochemically polymerized films. A review, Biosens. Bioelectron. 14 (1999) 443–456.
[22] N.C. Foulds, C.R. Lowe, Enzyme entrapment in electrically conducting polymers. Immobilisation of glucose oxidase in polypyrrole and its application in amperometric glucose sensors, J. Chem. Soc. Faraday Trans. 1 82 (1986) 1259–1264.
[23] R. Monošík, M. Stred'anský, E. Šturdík, Biosensors — classification, characterization and new trends, Acta Chim. Slov. (2012) 109.
[24] J. Pei, X.-y. Li, Amperometric glucose enzyme sensor prepared by immobilizing glucose oxidase on CuPtCl6 chemically modified electrode, Electroanalysis 11 (1999) 1266–1272.
[25] C.R. Martin, Template synthesis of electronically conductive polymer nanostructures, Acc. Chem. Res. 28 (1995) 61–68.
[26] S.K. Chakarvarti, J. Vetter, Template synthesis—a membrane based technology for generation of nano-/micro materials: a review, Radiat. Meas. 29 (1998) 149–159.
[27] R. Xiao, S.I. Cho, R. Liu, S.B. Lee, Controlled electrochemical synthesis of conductive polymer nanotube structures, J. Am. Chem. Soc. 129 (2007) 4483–4489.
[28] I. Otsuka, M. Yaoita, S. Nagashima, M. Higano, Molecular dimensions of dried glucose oxidase on a Au(111) surface studied by dynamic mode scanning force microscopy, Electrochim. Acta 50 (2005) 4861–4867.
[29] H.J. Hecht, H.M. Kalisz, J. Hendle, R.D. Schmid, D. Schomburg, Crystal structure of glucose oxidase from *Aspergillus niger* refined at 2 · 3 Å resolution, J. Mol. Biol. 229 (1993) 153–172.
[30] Huangxian Ju, X. Z., Joseph Wang. (2011) Nanobiosensing: Principles, Development and Application. ed. Springer, New York, USA.
[31] Small, E. W. (1991) Topics in Fluorescence Spectroscopy. ed. Plenum, Newyork.
[32] B. Ding, M. Wang, X. Wang, J. Yu, G. Sun, Electrospun nanomaterials for ultrasensitive sensors, Mater. Today 13 (2010) 16–27.
[33] Vasudevan, D. M. and Sreekumari, S. (2005) Textbook of biochemistry for medical students. ed. Jaypee Brothers Medical Publishers, New Delhi.
[34] Wilson, K. and Walker, J. M. (2005) Principles and techniques of biochemistry and molecular biology. ed. Cambridge University Press, United Kingdom.
[35] K. Dalziel, Physical significance of Michaelis constants, Nature 196 (1962) 1203–1205.
[36] R. Eisenthal, A. Cornish-Bowden, The direct linear plot. A new graphical procedure for estimating enzyme kinetic parameters, Biochem. J. 139 (1974) 715–720.
[37] J.T. Holland, J.C. Harper, P.L. Dolan, M.M. Manginell, D.C. Arango, J.A. Rawlings, C.A. Apblett, S.M. Brozik, Rational redesign of glucose oxidase for improved catalytic function and stability, PLoS One 7 (2012) e37924.
[38] Kotz, J. C. and Purcell, K. F. (1987) Chemistry & chemical reactivity ed. Saunders College Pub., Philadelphia.
[39] J. Heinze, B.A. Frontana-Uribe, S. Ludwigs, Electrochemistry of conducting polymers—persistent models and new concepts, Chem. Rev. 110 (2010) 4724–4771.
[40] T. Hernández-Pérez, M. Morales, N. Batina, M. Salmón, Effect of the electrosynthesis method on the surface morphology of the polypyrrole film an atomic force microscopy study, J. Electrochem. Soc. 148 (2001) C369–C375.
[41] J. Tietje-Girault, C. Ponce de León, F.C. Walsh, Electrochemically deposited polypyrrole films and their characterization, Surf. Coat. Technol. 201 (2007) 6025–6034.
[42] S. Brunauer, P.H. Emmett, E. Teller, Adsorption of gases in multimolecular layers, J. Am. Chem. Soc. 60 (1938) 309–319.
[43] D.P. Dubal, S.V. Patil, G.S. Gund, C.D. Lokhande, Polyaniline–polypyrrole nanograined composite via electrostatic adsorption for high performance electrochemical supercapacitors, J. Alloys Compd. 552 (2013) 240–247.
[44] L. Cao, Carrier-bound Immobilized Enzymes, Wiley-VCH Verlag GmbH & Co. KGaA 2006, pp. 1–52.
[45] J. Wang, N.V. Myung, M. Yun, H.G. Monbouquette, Glucose oxidase entrapped in polypyrrole on high-surface-area Pt electrodes: a model platform for sensitive electroenzymatic biosensors, J. Electroanal. Chem. 575 (2005) 139–146.
[46] B.E. Raabo, T.C. Terkildsen, On the enzymatic determination of blood glucose, Scand. J. Clin. Lab. Investig. 12 (1960) 402–407.
[47] G. Fu, Z. Dai, Efficient immobilization of glucose oxidase by in situ photo-cross-linking for glucose biosensing, Talanta 97 (2012) 438–444.
[48] G.Q. Xu, J. Lv, Z.X. Zheng, Y.C. Wu, Polypyrrole (PPy) nanowire arrays entrapped with glucose oxidase biosensor for glucose detection, 7th IEEE International conference on Nano/Macro Engineered and Molecular Systems, IEEE, Kyoto, Japan 2012, pp. 511–514.
[49] L. Xu, Y. Zhu, X. Yang, C. Li, Amperometric biosensor based on carbon nanotubes coated with polyaniline/dendrimer-encapsulated Pt nanoparticles for glucose detection, Mater. Sci. Eng. C 29 (2009) 1306–1310.
[50] D. Zhai, B. Liu, Y. Shi, L. Pan, Y. Wang, W. Li, R. Zhang, G. Yu, Highly sensitive glucose sensor based on Pt nanoparticle/polyaniline hydrogel heterostructures, ACS Nano 7 (2013) 3540–3546.
[51] B. Thakur, C.A. Amarnath, S.N. Sawant, Pectin coated polyaniline nanoparticles for an amperometric glucose biosensor, RSC Adv. 4 (2014) 40917–40923.
[52] B. Sharma, S. Mandani, T.K. Sarma, Enzymes as bionanoreactors: glucose oxidase for the synthesis of catalytic Au nanoparticles and Au nanoparticle–polyaniline nanocomposites, J. Mater. Chem. B 2 (2014) 4072–4079.
[53] X. Jiang, J. Jiang, Y. Jin, E. Wang, S. Dong, Effect of colloidal gold size on the conformational changes of adsorbed cytochrome c: probing by circular dichroism, UV–visible, and infrared spectroscopy, Biomacromolecules 6 (2005) 46–53.
[54] S. Zhou, H. Peng, X. Yu, X. Zheng, W. Cui, Z. Zhang, X. Li, J. Wang, J. Weng, W. Jia, F. Li, Preparation and characterization of a novel electrospun spider silk fibroin/poly(D, L-lactide) composite fiber, J. Phys. Chem. B 112 (2008) 11209–11216.
[55] X. Xu, P. Wu, W. Xu, Q. Shao, L. An, H. Zhang, C. Cai, B. Zhao, Effects of guanidinium ions on the conformational structure of glucose oxidase studied by electrochemistry, spectroscopy, and theoretical calculations: towards developing a chemical-induced protein conformation assay, Phys. Chem. Chem. Phys. 14 (2012) 5824–5836.
[56] E. Goormaghtigh, J.-M. Ruysschaert, V. Raussens, Evaluation of the information content in infrared spectra for protein secondary structure determination, Biophys. J. 90 (2006) 2946–2957.
[57] E. Serefoglou, K. Litina, D. Gournis, E. Kalogeris, A.A. Tzialla, I.V. Pavlidis, H. Stamatis, E. Maccallini, M. Lubomska, P. Rudolf, Smectite clays as solid supports for immobilization of β-glucosidase: synthesis, characterization, and biochemical properties, Chem. Mater. 20 (2008) 4106–4115.